Published OnlineFirst September 30, 2010; DOI: 10.1158/0008-5472.CAN-10-2460

Cancer Research

Acquired *TNFRSF14* Mutations in Follicular Lymphoma Are Associated with Worse Prognosis

K-John J. Cheung[1], Nathalie A. Johnson[1], Joslynn G. Affleck[2], Tesa Severson[5], Christian Steidl[1], Susana Ben-Neriah[1], Jacqueline Schein[5], Ryan D. Morin[5], Richard Moore[5], Sohrab P. Shah[3], Hong Qian[5], Jessica E. Paul[5], Adele Telenius[1], Thomas Relander[1], Wan Lam[4], Kerry Savage[1], Joseph M. Connors[1], Carolyn Brown[2], Marco A. Marra[5], Randy D. Gascoyne[1], and Douglas E. Horsman[1]

Abstract

Clinical correlative studies have linked 1p36 deletions with worse prognosis in follicular lymphoma (FL). In this study, we sought to identify the critical gene(s) in this region that is responsible for conferring inferior prognosis. BAC array technology applied to 141 FL specimens detected a minimum region of deletion (MRD) of ~97 kb within 1p36.32 in 20% of these cases. Frequent single-nucleotide polymorphism–detected copy-neutral loss of heterozygosity was also found in this region. Analysis of promoter CpGs in the MRD did not reveal differential patterns of DNA methylation in samples that differed in 1p36 status. Exon sequencing of MRD genes identified somatic alterations in the *TNFRSF14* gene in 3 of 11 selected cases with matching normal DNA. An expanded cohort consisting of 251 specimens identified 46 cases (18.3%) with nonsynonymous mutations affecting *TNFRSF14*. Overall survival (OS) and disease-specific survival (DSS) were associated with the presence of *TNFRSF14* mutation in patients whose overall treatment included rituximab. We further showed that inferior OS and DSS were most pronounced in patients whose lymphomas contained both *TNFRSF14* mutations and 1p36 deletions after adjustment for the International Prognostic Index [hazard ratios of 3.65 (95% confidence interval, 1.35–9.878, $P = 0.011$) and 3.19 (95% confidence interval, 1.06–9.57, $P = 0.039$), respectively]. Our findings identify *TNFRSF14* as a candidate gene associated with a subset of FL, based on frequent occurrence of acquired mutations and their correlation with inferior clinical outcomes.

Cancer Res; 70(22); 9166–74. ©2010 AACR.

Introduction

Follicular lymphoma (FL) is characterized at the karyotype level by the t(14;18)(q32;q21) translocation, which leads to overexpression of the antiapoptotic gene *BCL2* due to relocation in proximity to the *IGH* enhancer (1–6). In the great majority of cases, additional chromosomal changes are evident, some of which represent disease-associated events of clonal evolution. Alterations resulting in deletion of chromosome band 1p36 constitute the most frequent of these secondary karyotypic alterations. The 1p36 region has been the focus of attempts to refine the deletion breakpoints and identify driver or tumor suppressor gene(s), but historically, these efforts have been hampered by relatively small sample cohorts, the inclusion of heterogeneous subtypes of lymphoma, and the low resolution of analytic tools available including standard cytogenetic analysis and chromosome-based comparative genomic hybridization (CGH). Most of these studies have reported 1p36 aberrations in the form of intrachromosomal deletions and unbalanced translocations (7–10). Recently developed high-resolution technologies have shed further light on the issue. Of interest, a study by Ross and colleagues (5) of 58 FL cases analyzed using a 50k single-nucleotide polymorphism (SNP) array showed that 50% of these cases had either copy number loss or copy-neutral loss of heterozygosity (cnLOH) at 1p36. O'Shea and colleagues (11), using a lower-resolution 10k SNP assay, found 8% of cases to show cnLOH but found no evidence of deletions, possibly because of the low-resolution capability of the array; however, correlation between 1p36 cnLOH and overall survival (OS) was significant. These studies have highlighted the importance of alternate mechanisms of gene inactivation that may be operative in FL. Although the affected region of alteration identified in these studies was still relatively large at 8.5 Mb (5), a specific candidate gene was not identified.

In a previous study we have shown by karyotype and array CGH that a region of ~11 Mb from 1p36.22 to p36.33 was deleted at a frequency of ~25% in 106 FL specimens, and the deletion was shown to correlate with risk for development

Authors' Affiliations: [1]Center for Lymphoid Cancer, British Columbia Cancer Agency; Departments of [2]Medical Genetics, [3]Computer Science, and [4]Cancer Genetics and Developmental Biology, University of British Columbia; and [5]Genome Sciences Center, British Columbia Cancer Research Center, Vancouver, British Columbia, Canada

Note: Supplementary data for this article are available at Cancer Research Online (http://cancerres.aacrjournals.org/).

Corresponding Author: K-John J. Cheung, Center for Lymphoid Cancer, British Columbia Cancer Agency, 600 West 10th Avenue, Vancouver, British Columbia, Canada V5Z 4E6. Phone: 780-708-6425; Fax: 604-877-6089; E-mail: kjcheungjr@bccancer.bc.ca.

doi: 10.1158/0008-5472.CAN-10-2460

Published OnlineFirst September 30, 2010; DOI: 10.1158/0008-5472.CAN-10-2460

of transformed diffuse large B-cell lymphoma (DLBCL) and for poor survival outcome independent of clinical risk predictors (6). In this study, we have applied tiling path BAC array CGH, with a resolution of 80 to 150 kb (12), to a larger cohort of 141 FL specimens and applied robust computational algorithm to further fine-map the 1p36 deleted region. We have also used a custom-designed oligonucleotide microarray targeted to band 1p36, promoter methylation analysis, and exon sequencing to identify the potential gene of interest. Further, in an expanded cohort of 251 FL patients, we have assessed the frequency and clinical effect of somatic mutations of a candidate gene in the 1p36 region.

Materials and Methods

Patient materials

For breakpoint mapping of 1p36 deletions, 141 FL cases were selected from the Lymphoid Cancer Database of the British Columbia Cancer Agency, who were diagnosed between 1987 and 1996 based on the availability of sufficient frozen tumor material for DNA extraction. Of these 141 cases, 103 were included in a previous study (6). For the assessment of mutation frequency and clinical correlative analysis, we included 115 of the 141 cohort plus 136 additional specimens from our archive, totaling 251 cases with sufficient DNA for sequencing analysis. Each case had a lymph node biopsy containing FL obtained at the time of diagnosis or before systemic therapy and available clinical information that included initial clinical characteristics, age, stage, lactate dehydrogenase level, performance status, number of extranodal sites, treatment regimen, and clinical outcome (Table 1). It should be noted that the two cases with homozygous deletion of *TNFRSF14* were not included in the 251-patient cohort because there were insufficient follow-up data for survival analysis. Of these 251 patients, 35 had paired biopsies taken at the time of diagnosis and at transformation to aggressive DLBCL. The samples were accrued over a 20-year period (March 16, 1987 to September 11, 2007), reviewed by an expert hematopathologist (R.D.G.), and classified according to 2008 WHO criteria (13). Treatment regimens evolved over the 20 years and included observation, localized radiation, and systemic chemotherapy with or without rituximab, including rituximab maintenance. Chemotherapeutic regimens ranged from single-agent fludarabine and chlorambucil to multiagent

Table 1. Patient characteristics of the 251-FL-patient cohort

Clinical characteristics	Mutated, *n* = 46 (%)	Wild-type, *n* = 205 (%)	*P*
Male sex	21 (46)	114 (56)	0.4
Age >60 y	22 (49)	81 (39)	0.237
PS >1	11 (24)	21 (10)	0.009
LDH >normal	10 (22)	35 (17)	0.407
Extranodal sites >1	9 (20)	13 (6)	0.003
Stage III/IV	33 (73)	137 (67)	0.375
IPI score			
0–1	21 (47)	124 (60)	0.001
2–3	17 (38)	77 (37)	
4–5	7 (15)	5 (3)	
Diagnostic pathology			
Follicular, grade 1	24 (53)	123 (60)	0.670
Follicular, grade 2	15 (33)	56 (27)	
Follicular, grade 3	6 (13)	27 (13)	
Absence of translocation t(14;18)	2 (4)	25 (12)	
Absence of BCL2 expression	6 (13)	33 (16)	0.786
Treatment			
Observation/radiation alone	9 (20)	58 (28)	0.352
Chemo	14 (31)	38 (18)	
Chemo + ritux*	15 (33)	79 (38)	
Chemo + ritux + ritux maintenance	7 (16)	31 (16)	
Outcome			
Transformation	13 (29)	58 (28)	
Death	18 (40)	51 (25)	
Median follow up of living patients = 3 y			

Abbreviations: Mut, *TNFRSF14* mutation; PS, Eastern Cooperative Oncology Group performance status; LDH, lactate dehydrogenase; chemo, chemotherapy; ritux, rituximab.

*Eleven of 15 (73%) as first-line therapy in the Mutated cohort, and 59 of 79 (75%) as first-line therapy in the Wild-type cohort.

Published OnlineFirst September 30, 2010; DOI: 10.1158/0008-5472.CAN-10-2460

regimens such as CVP (cyclophosphamide, vincristine, and prednisone) or CHOP (cyclophosphamide, doxorubicin, vincristine, and prednisone). Information on the percentages of patients receiving rituximab as part of their first-line therapy is listed in Table 1. This study was approved by the University of British Columbia-British Columbia Cancer Agency Research Ethics Board.

Cytogenetic analysis

Cytogenetic analysis of lymph node specimens was performed as previously described (8). Fluorescence *in situ* hybridization (FISH) was performed on residual cell suspensions using the LSI *IGH/BCL2* probe according to the manufacturer's protocol (Vysis) to detect the presence of *IGH/BCL2* genomic fusion. For validation of deletion of the 1p36.32 locus, the BAC clones RP13-493G06, RP13-586E24, and RP11-756P03 were selected from the array CGH profile and prepared for use as FISH probes as previously described (14). BAC RP11-229M05 at 1q32.3 was used as a copy number control. All BAC clones had previously been identity-verified by BAC-end sequencing and by hybridization to normal metaphases to confirm the expected site of chromosomal localization. The frequency of false deletion for each BAC FISH probe was established by hybridization to normal lymphocyte cell suspensions and ranged from 0.5% to 3.0%. For the purpose of this study, the cutoff value for true deletion was set at >5% of 200 interphase nuclei. All of the FISH studies were performed on residual methanol/acetic acid–preserved cell pellets.

Sample preparation

Genomic tumor DNA was extracted from frozen tissues or frozen cell suspensions using the ALLPREP kit (Qiagen). Germline DNA was extracted from peripheral blood in 11 patients using the PureGene DNA purification kit (Gentra).

BAC array CGH and oligonucleotide array analysis

The sub-megabase resolution tiling (SMRT) BAC array contains 26,819 BAC clones spotted in duplicate on glass slides and covers >95% of the human genome (15, 16). Array CGH using this platform was performed as previously described (17). A custom-built high-density Agilent oligonucleotide array was designed using the eArray software (Agilent Technologies) and contained ~12,000 60-mer probes with an average of one probe per 500 bp spanning the first 5,983,478 bp of the 1p terminus. Hybridization to the custom Agilent array was performed using 500 ng of tumor DNA according to the manufacturer's protocol (Agilent Technologies). Analysis of BAC array CGH data was performed using the joint inference Hidden Markov Model called Conditional Markov Model (CMM) proposed by Colella and colleagues, adapted for array CGH to detect subtle clone shifts in recurrent cases (18). The model consists of a nonstationary transition matrix indexed by a probe that is shared across samples, thus allowing for borrowing statistical strength that may be present in recurrent alterations. Data from the Agilent oligo array were visualized using the CGHAnalytics 3.0 software (Agilent Technologies) and analyzed using the supplied statistical algorithm ADM-1, with the sensitivity threshold set to 5.0, the moving average window to 1 Mb, and the requirement of 10 consecutive probes to annotate a loss or a gain.

DNA methylation analysis

CpG's were selected for pyrosequencing based on their location within the promoter of the associated gene. Specifically, if the gene had a CpG island promoter, CpG's from within the island were chosen. If the gene did not have an identified CpG island promoter, CpG's closest to the transcription start site were chosen. PCR primer and sequencing primer design were performed using the PyroMark software (Qiagen). Genomic DNA (500 ng) was bisulfite-converted using the EZ DNA Methylation Gold Kit (Zymo Research Corporation) according to the manufacturer's protocol. Cycling conditions were as follows: 95°C for 15 minutes, 50 cycles of [94°C for 30 seconds, 57°C for 30 seconds, and 72°C for 1 minute], 72°C for 10 minutes. PCR products were then prepared for pyrosequencing as described by Tost and Gut (19) using the PyroMark reagent kit (Qiagen) and sequencing primers as listed in Supplementary Table S1. Pyrosequencing was performed using a PyroMark Q96 ID instrument (Qiagen) and bisulfite DNA conversion was confirmed using internal bisulfite conversion controls.

DNA sequencing

Exon sequencing was performed using an ABI 3730xl DNA analyzer and the Jumpstart Taq DNA polymerase (Sigma-Aldrich) according to the manufacturer's instructions. Each amplification primer set was tagged with M13F(-21) forward (5′-TGTAAAACGACGGCCAGT-3′) and M13 reverse (5′-CAGGAAACAGCTATGAC-3′) for direct sequencing. Cycling conditions were as follows: 94°C for 1 minute, 30 cycles of 98°C for 10 seconds, 68°C for 6 minutes, and 72°C for 10 minutes. Mutation Surveyor software (SoftGenetics LLC) was used to analyze the sequence data. Information on primer sequences is provided in Supplementary Table S1.

Statistical analysis

Statistical analyses were performed using SPSS Software version 14.0. For methylation analysis, differences among groups were evaluated by one-way ANOVA. Pearson's χ^2 test was used to determine the significance of any differences between the clinical variables in mutated versus wild-type samples. Survival curves were plotted using the Kaplan-Meier method and compared using the log-rank test. OS was defined as the time from diagnosis to date of most recent follow-up (censored) or death from any cause (event). The Cox proportional hazards model that included the International Prognostic Index (IPI) score was used to determine the significance of variables in the univariate survival analyses. All statistical tests were two-sided and considered significant at $P \leq 0.05$.

Results

Identification of the minimum region of deletion on 1p36

In a previous study we showed a deletion frequency of ~25% at chromosome band 1p36 based on the BAC array

Published OnlineFirst September 30, 2010; DOI: 10.1158/0008-5472.CAN-10-2460

CGH analysis of 106 diagnostic FL biopsies (6). Herein we report a frequency of 20% in 141 FL cases using an algorithm called CMM joint analysis that identified a minimum region of deletion (MRD) corresponding to a single BAC clone with the highest frequency shift (Fig. 1A). This area is approximately 97 kb in size and contains five genes including *HES5, LOC115110, TNFRSF14, C1orf93*, and *MMEL1*. Information on the BAC clone within the MRD and the frequency of loss, gain, and copy-neutral state is shown in Fig. 1A (bottom).

Figure 1B (right) shows four representative array CGH cases with heterozygous (–/+) and homozygous (–/–) deletions and the corresponding FISH profiles (1p36: red arrowhead; 1q32 control: green arrowhead). All deletions detected by array CGH were validated by FISH analysis using one or more of the BAC probes RP13-493G06, RP13-586E24, and RP11-756P03 with probe RP11-229M05 mapping at 1q32.3 as a copy number control. The majority of the deletions were shown to be heterozygous, whereas two were homozygous. High-resolution oligonucleotide array analysis was performed on case 1, which had the smallest array CGH–detected 1p36 deletion, to fine-map the breakpoints (Fig. 1B, left). Due to numerous sequence repeats in this area, a portion of the deleted region was not covered by the probes; however, the deletion spanned 224,674 bp containing the five genes identified in the MRD by array CGH analysis (red/black/blue dots are data points representing gain/neutral/loss status).

The MRD region was also examined with Affymetrix mapping 500k SNP arrays to detect possible cnLOH using 27 selected cases with available matched germline DNA (from the 141 cases used to determine the MRD). Six of the 27 cases (22.2%) showed cnLOH affecting chromosome arm 1p with an overlapping region of cnLOH of approximately 15Mb that included the 97-kb MRD identified by array CGH (data not shown).

Methylation status of genes in the MRD

The methylation pattern of four of the five genes within the MRD was investigated using the pyrosequencing technique (Fig. 2). Technical failures prevented the analysis of *LOC115110*, likely owing to abundant sequence repeats in the promoter region (see Fig. 2). A number of samples were not investigated because of the lack of available tumor DNA.

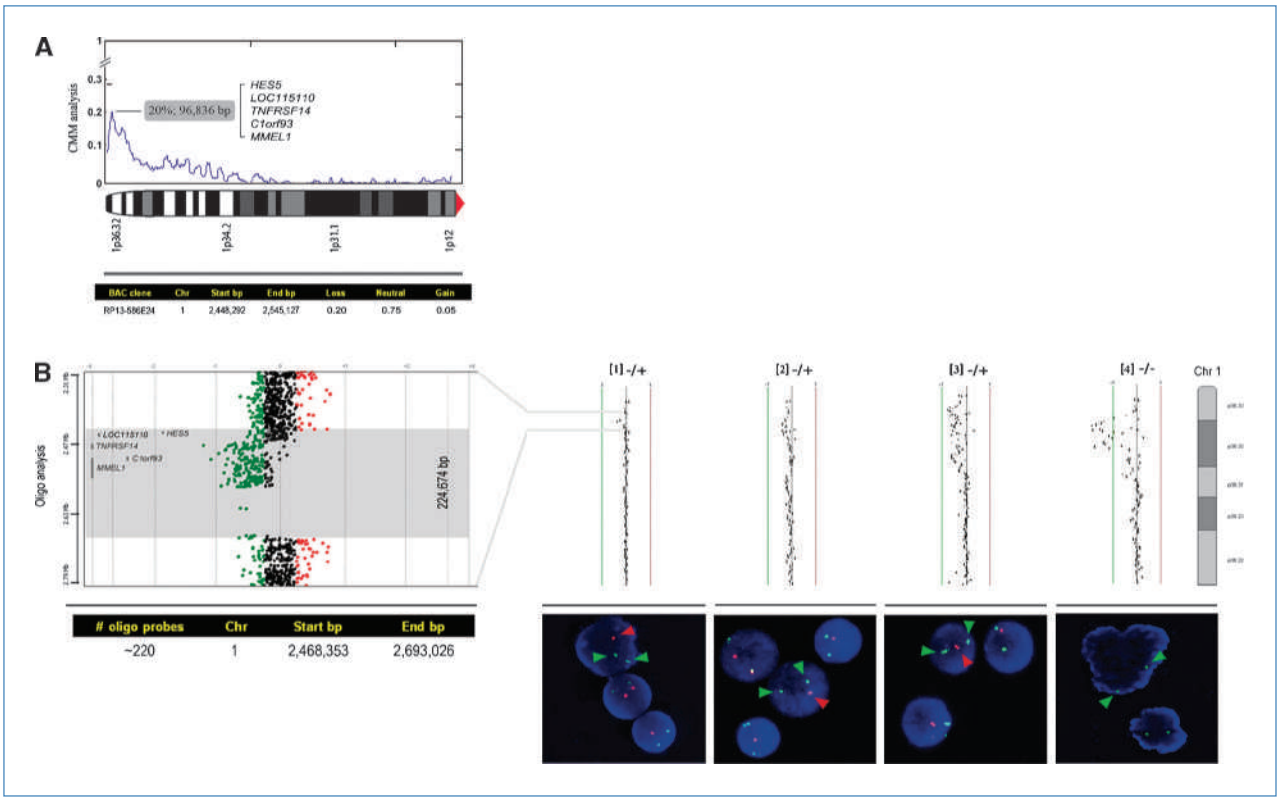

Figure 1. 1p36 MRD identification. A, array CGH composite deletion frequency profile of chromosome arm 1p in 141 FL patients. Analysis using the CMM algorithm produced a graph showing an MRD in band 1p36.32 with the highest frequency of loss corresponding to BAC clone RP13-586E24, which contains the genes *HES5, LOC115110, TNFRSF14, C1orf93*, and *MMEL1*. *Y*-axis, probability of aberrations; *X*-axis, chromosome band coordinates. Associated information for BAC clone RP13-586E24 is presented below the graph. B, right, four representative array CGH cases are shown with heterozygous (–/+) and homozygous deletions (–/–) and the corresponding FISH profiles (red arrowhead, 1p36; green arrowhead, 1q32 control). Left, custom oligo array analysis of case 1 showing left shift from the center line, indicating deletion of ~224 kb (red/black/blue dots are data points representing gain/neutral/loss status). Chr, chromosome.

Published OnlineFirst September 30, 2010; DOI: 10.1158/0008-5472.CAN-10-2460

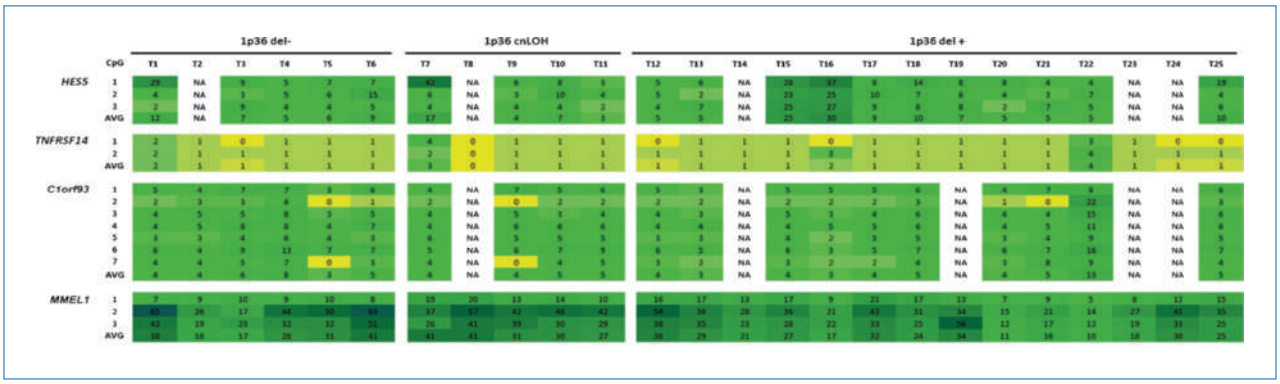

Figure 2. Methylation analysis. Six specimens (T1–T6) without 1p36 deletions (1p36 del–), five specimens (T7–T11) with 1p36 cnLOH, and 14 specimens (T12–T25) with 1p36 deletions (1p35 del+) were examined. The number of CpGs analyzed is indicated beside each gene. The percent methylation is presented numerically and by color coding (yellow, least; green, intermediate; blue, highly). NA, not available.

The number of CpG dinucleotides analyzed at each gene promoter is indicated beside each gene in Fig. 2. The percent methylation of each CpG is presented both numerically and by color coding (with yellow being the least methylated, green being intermediate, and blue being highly methylated). None of the genes examined showed a differential methylation pattern among (*a*) six cases without array CGH–detected 1p36 deletion (1p36 del–), (*b*) five cases with cnLOH (1p36 cnLOH), and (*c*) 14 cases with 1p36 deletion (1p36 del+; $P > 0.05$, one-way ANOVA).

Identification of somatic mutations in *TNFRSF14*

Exon sequencing of the five genes identified within the MRD was performed on 11 cases: 5 cases with and 6 cases without deletion of 1p36 as determined by array CGH analysis. We searched for somatic mutations in the sequence data from the lymphoma cells by comparison with constitutional DNA obtained from peripheral blood lymphocytes from the same patient. The exons and exon/intron boundaries for *HES5* (exons 1–3), *LOC115110* (exons 1 and 2), *TNFRSF14* (exons 1–8), *C1orf93* (exons 1–7), and *MMEL1* (exons 18–23) were studied. Exons 1 to 17 and 24 of *MMEL1* could not be covered by PCR amplicons owing to high content of GC repeats; therefore, the existence of mutations in these exons cannot be excluded. Of the five genes, only *TNFRSF14* displayed somatic mutations. Four somatic mutations were found in the tumor DNA from three of the five cases with 1p36 deletion. One case had an A > G transition in exon 1 resulting in an amino acid change from methionine to valine, plus a synonymous change from G > A also in exon 1. Another case had a G > T transversion in exon 2 resulting in truncation. The last case had a G > A transition in the first base of intron 4. There were no somatic mutations detected in the six cases without a 1p36 deletion.

Validation of *TNFRSF14* mutation frequency and correlation with inferior prognosis

To determine the frequency of *TNFRSF14* mutation and to undertake clinical correlative analysis, we selected 115 cases with sufficient DNA from our 141 discovery cohort (used in determining the MRD and for which 1p36 deletion status was known) plus 136 additional FL specimens from our archive in which 1p36 deletion status was not known, totaling 251 primary FL cases. The clinical features and mutation findings for these cases are summarized in Tables 1 and 2, respectively. Briefly, in 46 cases (18.3%), we identified a total of 47 previously undescribed nonsynonymous mutations in *TNFRSF14* after screening to exclude known polymorphic variants using several databases including NCBI dbSNP Build 130 (http://www.ncbi.nlm.nih.gov/projects/SNP/), J. Craig Venter HuRef Genome Browser (http://huref.jcvi.org/), James Watson Genotype Viewer (http://jimwatsonsequence.cshl.edu/cgi-perl/gbrowse/jwsequence/), and the 1000 Genomes Project (http://www.1000genomes.org/page.php). The 47 nonsynonymous mutations included 22 transitions, 13 transversions, 8 deletions, and 4 insertions resulting in 16 truncations and 10 frameshifts (Table 2). All exons except 7 and 8 were affected by mutations. One case showed two mutations in *TNFRSF14*.

On examination of the relationship between 1p36 deletion and *TNFRSF14* mutation among the 114 cases whose deletion status and mutation status were known, we found that 8 cases (7%) were positive for both 1p36 deletion and *TNFRSF14* mutation, 10 cases (8.8%) were *TNFRSF14* mutation positive and 1p36 deletion negative, and 23 cases (20.2%) were 1p36 deletion positive and *TNFRSF14* mutation negative. The clinical effect of these findings is presented below. Furthermore, we found that among the 35 cases with paired specimens taken at diagnosis and later at the time of development of transformed DLBCL, a *TNFRSF14* mutation was detected in both samples from five paired specimens and in two of the transformed samples whose corresponding prior FL samples had no mutation.

Analysis of clinical correlation with *TNFRSF14* mutations in an expanded cohort of 251 cases revealed that *TNFRSF14* mutations were associated with high-risk clinical features (see Table 1). Specifically, patients with mutated *TNFRSF14* were more likely to have a poor performance status, and their FL involved a greater number of extranodal sites. When patients whose overall treatment included rituximab were

Published OnlineFirst September 30, 2010; DOI: 10.1158/0008-5472.CAN-10-2460

analyzed, inferior OS and disease-specific survival (DSS) were observed in those with a mutation in *TNFRSF14* (median of 3.73 and 7.52 years, respectively) compared with those without (median of 15.85 and 15.85 years; log-rank test, $P < 0.001$ and $P = 0.004$, respectively; Fig. 3A and B). On multivariate analysis using Cox regression, *TNFRSF14* mutation emerged as a stronger predictor of inferior OS and DSS after adjustment for the IPI in rituximab-treated patients {hazard ratios

Table 2. Information on the 47 nonsynonymous mutations in the *TNFRSF14* gene

Chr1 position	Exon	Transcript position: alteration	Amino acid position: alteration
2486246	1	368:het_delG	23:deletion/frameshift
2486260	1	354:G>C	19:D>H:transversion
2486272	1	342 to 346:het_delACCCC	15:deletion/frameshift
2486274	1	340 to 344:het_delCCACC	14:deletion/frameshift
2486279	1	335:G>A	12:W>X:transition/truncation
2486280	1	334:G>A	12:W>X:transition/truncation
2486295	1	319:G>A	7:W>X:transition/truncation
2486312	1	302:G>A	1:M>I:transition
2486312	1	302:G>A	1:M>I:transition
2486314	1	300:A>T	1:M>L:transversion
2485148	2	1466:C>T	59:P>S:transition
2485152	2	1462:C>A	57:C>X:transversion/truncation
2485182	2	1432:C>A	47:Y>X:transversion/truncation
2485197	2	1417:C>G	42:C>W:transversion
2485197	2	1417:C>G	42:C>W:transversion
2485224	2	1390 to 1391:het_insC	34:insertion/frameshift
2485230	2	1384 to 1385:het_insC	32:insertion/frameshift
2485245	2	1369:T>A	26:Y>X:transversion/truncation
2485247	2	1367:T>A	26:Y>N:transversion
2485249	2	1365:T>G	25:L>R:transversion
2484526	3	2088:C>T	97:Q>X:transition/truncation
2484571	3	2043:A>C	82:T>P:transversion
2484583	3	2031:T>C	78:C>R:transition
2484590	3	2024 to 2025:delTG	75:deletion/frameshift
2484600	3	2014:G>A	72:G>D:transition
2484622	3	1992:G>T	65:E>X:transversion/truncation
2484633	3	1981:A>G	61:Y>C:transition
2484636	3	1978:G>A	60:G>D:transition
2483010	4	3604:C>T	151:Q>X:transition/truncation
2483012	4	3602 to 3611:het_delTGCAGAAGGG	150:deletion/frameshift
2483019	4	3595:C>T	148:Q>X:transition/truncation
2483050	4	3564 to 3567:het_delGTGC	137:deletion/frameshift
2483056	4	3558 to 3567:het_delCGCCGCGTGC	136:deletion/frameshift
2483086	4	3528 to 3529:het_insGCCGTGTGTGGCTGCAGCCCAGGCCAC	126:insertion
2483099	4	3515:G>A	121:C>Y:transition
2483116	4	3498 to 3499:het_insACACCGTGTGTGGCTGCAGCCCAGGCC	116:insertion
2483136	4	3478:C>T	109:R>W:transition
2482330	5	4284:T>A	162:C>X:transversion/truncation
2482344	5	4270:C>T	158:Q>X:transition/truncation
2481164	6	5450:G>A	232:G>S:transition
2481214	6	5400:T>A	215:V>D:transversion
2481246	6	5368:G>A	204:W>X:transition/truncation
2481249	6	5365:G>A	203:W>X:transition/truncation
2481256	6	5358:G>A	201:W>X:transition/truncation
2481282	6	5332 to 5341:het_delCGGAGCTGGG	193:deletion/frameshift
2481297	6	5317:G>A	187:W>X:transition/truncation
2481297	6	5317:G>A	187:W>X:transition/truncation

Abbreviations: chr1, chromosome 1; >, mutated to; het_del, heterozygous deletion; het_ins, heterozygous insertion; X, stop codon.

Published OnlineFirst September 30, 2010; DOI: 10.1158/0008-5472.CAN-10-2460

[HR] of 4.54 [95% confidence interval (95% CI), 1.80–11.44; $P = 0.001$] and 3.97 [95% CI, 1.50–10.51; $P = 0.006$], respectively}. Where information was available, all patients were classified into groups based on the presence or absence of 1p36 deletion and/or *TNFRSF14* mutation. Patients with one alteration (mut or del"; median, 7.52 years) or both alterations ("mut/del"; median, 6.09 years) displayed a significantly inferior OS compared with those without either alteration ("no mut/no del"; median, 11.23 years) or cases without any mutation but in whom the 1p36 deletion status was unknown ("no mut/del NA"; median, 11.69 years; log-rank test, $P = 0.005$; see Fig. 3C). On multivariate analysis, cases with both aberrations (1p36 deletion and *TNFRSF14* mutation) remained a significant predictor of OS independent of the IPI compared with the group of no aberrations (HR, 3.65; 95% CI, 1.35–9.878; $P = 0.011$). In the analysis of DSS, patients with both alterations ("mut/del"; median, 7.61 years) displayed a significantly inferior DSS compared with those

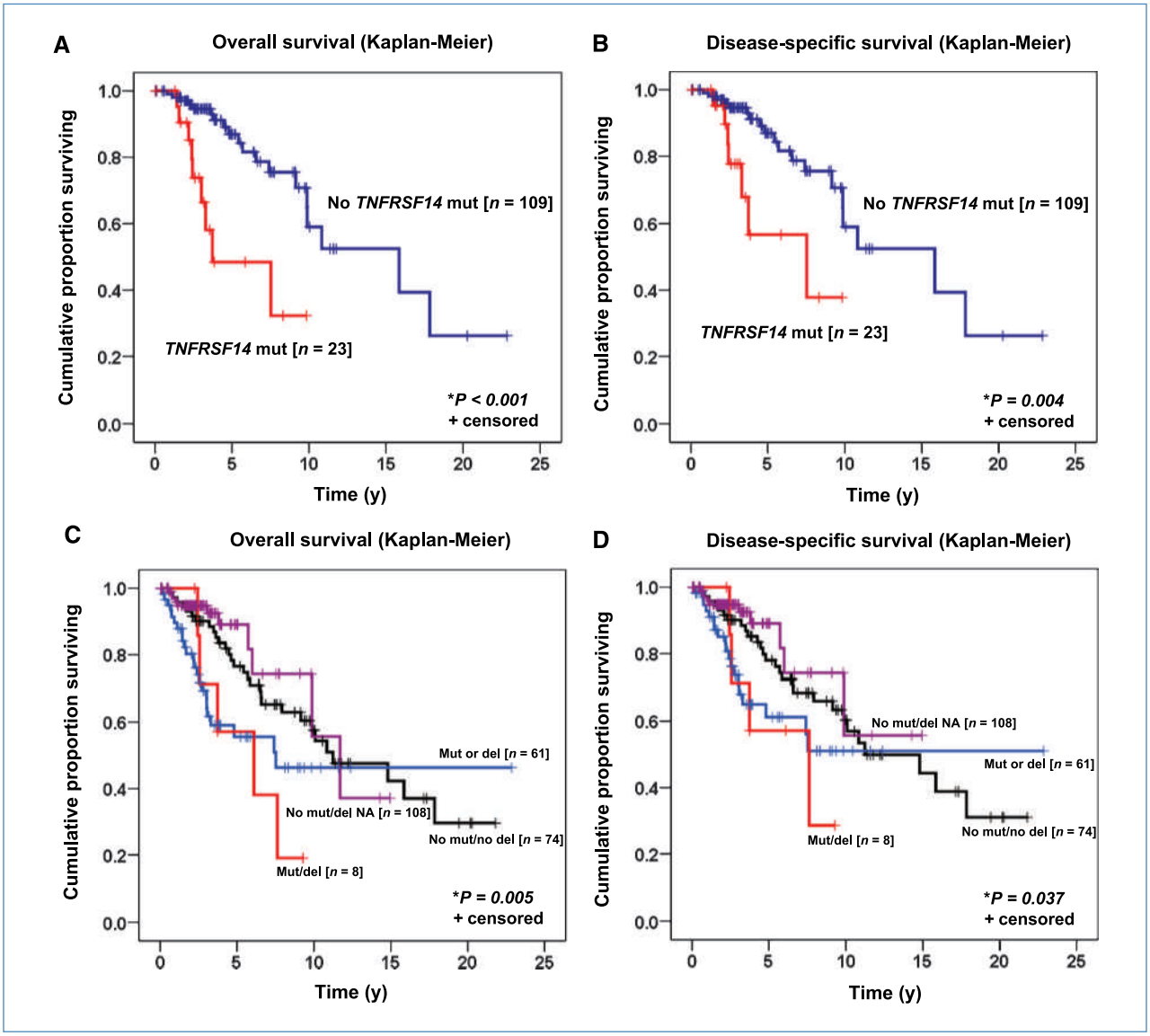

Figure 3. Clinical correlation analysis. A, OS according to the presence or absence of *TNFRSF14* mutation in rituximab-treated patients (median, 3.73 and 15.85 y, respectively; log-rank test, $P < 0.001$). B, DSS according to the presence or absence of *TNFRSF14* mutation in rituximab-treated patients (median, 7.52 and 15.85 y, respectively; log-rank test, $P = 0.004$). C, OS according to four categories: (*a*) the absence of *TNFRSF14* mutation and 1p36 deletion ("no mut/no del"; median, 11.32 y); (*b*) the absence of *TNFRSF14* mutation and information of 1p36 deletion not available ("no mut/del NA"; median, 11.69 y); (*c*) the presence of *TNFRSF14* mutation or 1p36 deletion ("mut or del"; median, 7.52 y); and (*d*) the presence of both *TNFRSF14* mutation and 1p36 deletion ("mut/del"; median, 6.09 y; log-rank test, $P = 0.005$). D, DSS according to four categories: (*a*) the absence of *TNFRSF14* mutation and 1p36 deletion ("no mut/no del"; median, 11.32 y); (*b*) the absence of *TNFRSF14* mutation and information of 1p36 deletion not available ("no mut/del NA"; median not reached); (*c*) the presence of *TNFRSF14* mutation or 1p36 deletion ("mut or del"; median not reached); and (*d*) the presence of both *TNFRSF14* mutation and 1p36 deletion ("mut/del"; median, 7.61 y; log-rank test, $P = 0.037$).

Published OnlineFirst September 30, 2010; DOI: 10.1158/0008-5472.CAN-10-2460

without either alteration ("no mut/no del"; median, 11.23 years), those with one alteration ("mut or del"; median not reached), or cases without any mutation but in whom the 1p36 deletion status was unknown ("no mut/del NA"; median not reached; log-rank test, $P = 0.037$; see Fig. 3D). Cases with both aberrations (1p36 deletion and *TNFRSF14* mutation) remained a significant predictor independent of the IPI compared with the group with no aberrations (HR, 3.19; 95% CI, 1.06–9.57; $P = 0.039$).

Discussion

Based on microarray-based copy number and cnLOH data analyses, we have identified a MRD at chromosome band 1p36 in FL that measures approximately 97 kb. This region contains five genes: *HES5, LOC115110, TNFRSF14, C1orf93*, and *MMEL1*. Direct DNA sequencing of the exons of these genes in the 11 cases with matching tumor and constitutional DNA revealed that only *TNFRSF14* was affected by acquired somatic mutations in the clonal cells. In the cohort of 251 cases where matching constitutional DNA was not examined, 47 nonsynonymous mutations were detected in 46 cases (18.3%; after elimination of known polymorphic variants). Although the mutations detected in the 251 case study were not definitively confirmed to be somatic by parallel constitutional DNA sequencing, the lack of similar mutations in large public genomic databases and the significant correlation of these observed mutations with inferior clinical outcomes provide strong evidence that these mutations are somatic in nature and that *TNFRSF14* is the target gene in the 1p36 MRD.

In the clinical correlative analysis of the 251-patient cohort, we report three interesting observations. First, patients with *TNFRSF14* mutations were more likely to have high-risk clinical features such as poor performance status and involvement of multiple extranodal sites. Second, *TNFRSF14* mutation alone or combined with 1p36 deletion correlated with inferior prognosis. Third, the adverse effect of *TNFRSF14* mutation on FL patients was independent of rituximab treatment. The implications of these findings are of clinical significance. Essentially, there seems to be a dose effect where homozygosity for a somatic *TNFRSF14* gene defect (deletion plus mutation) was correlated with the poorest clinical outcomes. In addition, treatment with rituximab conferred less-than-expected benefit in patients with a mutation in *TNFRSF14*. Furthermore, our observation that *TNFRSF14* mutations were detected in both the paired diagnostic and transformed specimens or only in transformed specimens suggests that *TNFRSF14* mutation may play a role in transformation of FL to DLBCL.

The *TNFRSF14* gene is located on the chromosome 1 minus DNA strand from base pairs 2,479,150 to 2,486,757 and is composed of eight exons, which together produce an RNA transcript 1,731 bp in size and a protein product consisting of 283 amino acids. The significance of such acquired mutations on the structure-function relationship of *TNFRSF14* is unclear; however, a previous study has found that alterations of amino acid residues at positions 14, 23, and 26 (corresponding to exons 1, 1, and 2, respectively) significantly reduce its binding affinity to BTLA, one of the protein ligands for TNFRSF14 in negatively modulating T-cell immune responses (20). Of interest in light of this report, we found one case with a frameshift mutation corresponding to amino acid position 14, another frameshift mutation corresponding to position 23, and a nonsynonymous mutation corresponding to position 26. Among the mutations detected in *TNFRSF14*, we found an exon-intron junction alteration. Because *TNFRSF14* can produce 15 different splice variants, alterations at splice sites will likely disrupt their recognition by the transcription machinery, leading to introns not being removed from the pre-mRNA and/or frameshifts (21, 22). *In vitro* investigation will be needed to further examine the effect of mutations on cellular function in different parts of the gene. Furthermore, CpG methylation analysis of the five genes in the MRD showed that acquired methylation was unlikely to be a mechanism involved in the transcriptional silencing of *TNFRSF14*.

In conclusion, we have identified a MRD at 1p36 that encompasses five genes, of which only *TNFRSF14* (also called *HVEA, HVEM, ATAR, TR2*, or *LIGHTR*) is associated with FL based on the presence of somatic mutations and the observation that FL patients with *TNFRSF14* mutation alone or combined with a 1p36 deletion have an inferior prognosis. To the best of our knowledge, no other studies have been able to provide strong evidence for a candidate gene in the 1p36 deleted region in FL. Although the physiologic role of *TNFRSF14* in humans is still being deciphered, recent evidence indicates that in addition to being a member of the TNF receptor superfamily, normal *TNFRSF14* is capable of inhibiting the proliferation of adenocarcinoma cells and enhancing Fas-induced apoptosis in non–Hodgkin's lymphoma cells, suggesting a tumor suppressor role (23, 24). Functional analysis of this gene, specifically the effect of mutations on the function of TNFRSF14, is the subject of ongoing investigations. The identification of *TNFRSF14* as a candidate gene in the second most frequently altered region in the FL genome will not only open the possibility of it being developed as a prognostic marker for identifying high-risk patients as candidates for risk-adapted therapies, but TNFRSF14 may also provide pharmacologic clues on why rituximab treatment in some cases of FL may have a less-than-expected beneficial effect on survival.

Disclosure of Potential Conflicts of Interest

No potential conflicts of interest were disclosed.

Acknowledgments

We thank Dr. Stephane Le Bihan, Anne Haegert, and Robert Bell from the Vancouver Prostate Center Microarray Facility for their Agilent oligo array services; A.M. Devlin for the use of pyrosequencing instruments; and Jane Donaldson and Suman Singh for maintenance of the BCCA Lymphoid Cancer Database.

Published OnlineFirst September 30, 2010; DOI: 10.1158/0008-5472.CAN-10-2460

Grant Support

Terry Fox Foundation New Frontiers Program Project Grant 019001 and Genome Canada/BC Grant Competition III (J.M. Connors, R.D. Gascoyne, and D.E. Horsman); National Cancer Institute of Canada grant 019005, Michael Smith Foundation for Health Research grant ST-PDF-01793, and Canadian Institute of Health Research grant STP-53912 (N.A. Johnson); Deutsche Forschungsgemeinschaft grant STE-1706/1-1 (C. Steidl). M.A. Marra is a Terry Fox Young Investigator and Michael Smith Senior Research Scholar.

The costs of publication of this article were defrayed in part by the payment of page charges. This article must therefore be hereby marked *advertisement* in accordance with 18 U.S.C. Section 1734 solely to indicate this fact.

Received 07/06/2010; revised 09/18/2010; accepted 09/22/2010; published OnlineFirst 09/30/2010.

References

1. Yunis JJ, Frizzera G, Oken MM, McKenna J, Theologides A, Arnesen M. Multiple recurrent genomic defects in follicular lymphoma. A possible model for cancer. N Engl J Med 1987;316:79–84.
2. Tilly H, Rossi A, Stamatoullas A, et al. Prognostic value of chromosomal abnormalities in follicular lymphoma. Blood 1994;84:1043–9.
3. Tsujimoto Y, Finger LR, Yunis J, Nowell PC, Croce CM. Cloning of the chromosome breakpoint of neoplastic B cells with the t(14;18) chromosome translocation. Science 1984;226:1097–9.
4. Graninger WB, Seto M, Boutain B, Goldman P, Korsmeyer SJ. Expression of Bcl-2 and Bcl-2-Ig fusion transcripts in normal and neoplastic cells. J Clin Invest 1987;80:1512–5.
5. Ross CW, Ouillette PD, Saddler CM, Shedden KA, Malek SN. Comprehensive analysis of copy number and allele status identifies multiple chromosome defects underlying follicular lymphoma pathogenesis. Clin Cancer Res 2007;13:4777–85.
6. Cheung KJ, Shah SP, Steidl C, et al. Genome-wide profiling of follicular lymphoma by array comparative genomic hybridization reveals prognostically significant DNA copy number imbalances. Blood 2009;113:137–48.
7. Lestou VS, Gascoyne RD, Sehn L, et al. Multicolour fluorescence *in situ* hybridization analysis of t(14;18)-positive follicular lymphoma and correlation with gene expression data and clinical outcome. Br J Haematol 2003;122:745–59.
8. Horsman DE, Connors JM, Pantzar T, Gascoyne RD. Analysis of secondary chromosomal alterations in 165 cases of follicular lymphoma with t(14;18). Genes Chromosomes Cancer 2001;30:375–82.
9. Lestou VS, Ludkovski O, Connors JM, Gascoyne RD, Lam WL, Horsman DE. Characterization of the recurrent translocation t(1;1)(p36.3;q21.1-2) in non-Hodgkin lymphoma by multicolor banding and fluorescence *in situ* hybridization analysis. Genes Chromosomes Cancer 2003;36:375–81.
10. Rajgopal A, Carr IM, Leek JP, et al. Detection by fluorescence *in situ* hybridization of microdeletions at 1p36 in lymphomas, unidentified on cytogenetic analysis. Cancer Genet Cytogenet 2003;142:46–50.
11. O'Shea D, O'Riain C, Gupta M, et al. Regions of acquired uniparental disomy at diagnosis of follicular lymphoma are associated with both overall survival and risk of transformation. Blood 2009;113:2298–301.
12. Garnis C, Coe BP, Lam SL, MacAulay C, Lam WL. High-resolution array CGH increases heterogeneity tolerance in the analysis of clinical samples. Genomics 2005;85:790–3.
13. Harris NL, Jaffe ES, Diebold J, et al. The World Health Organization classification of neoplasms of the hematopoietic and lymphoid tissues: report of the Clinical Advisory Committee meeting-Airlie House, Virginia, November, 1997. Hematol J 2000;1:53–66.
14. Henderson LJ, Okamoto I, Lestou VS, et al. Delineation of a minimal region of deletion at 6q16.3 in follicular lymphoma and construction of a bacterial artificial chromosome contig spanning a 6-megabase region of 6q16-21. Genes Chromosomes Cancer 2004;40:60–5.
15. Ishkanian AS, Malloff CA, Watson SK, et al. A tiling resolution DNA microarray with complete coverage of the human genome. Nat Genet 2004;36:299–303.
16. Davies JJ, Wilson IM, Lam WL. Array CGH technologies and their applications to cancer genomes. Chromosome Res 2005;13:237–48.
17. de Leeuw RJ, Davies JJ, Rosenwald A, et al. Comprehensive whole genome array CGH profiling of mantle cell lymphoma model genomes. Hum Mol Genet 2004;13:1827–37.
18. Colella S, Yau C, Taylor JM, et al. QuantiSNP: an objective Bayes Hidden-Markov Model to detect and accurately map copy number variation using SNP genotyping data. Nucleic Acids Res 2007;35:2013–25.
19. Tost J, Gut IG. DNA methylation analysis by pyrosequencing. Nat Protoc 2007;2:2265–75.
20. Compaan DM, Gonzalez LC, Tom I, Loyet KM, Eaton D, Hymowitz SG. Attenuating lymphocyte activity: the crystal structure of the BTLA-HVEM complex. J Biol Chem 2005;280:39553–61.
21. Mount SM. A catalogue of splice junction sequences. Nucleic Acids Res 1982;10:459–72.
22. Kahl U. 50 years after the discovery of the DNA structure its implications still have not reached clinical practice. Our genetic material is "a big tangle of nucleic acids and proteins". Lakartidningen 2003;100:2218–21.
23. Harrop JA, McDonnell PC, Brigham-Burke M, et al. Herpesvirus entry mediator ligand (HVEM-L), a novel ligand for HVEM/TR2, stimulates proliferation of T cells and inhibits HT29 cell growth. J Biol Chem 1998;273:27548–56.
24. Costello RT, Mallet F, Barbarat B, et al. Stimulation of non-Hodgkin's lymphoma via HVEM: an alternate and safe way to increase Fas-induced apoptosis and improve tumor immunogenicity. Leukemia 2003;17:2500–7.

AACR American Association for Cancer Research

Cancer Research

The Journal of Cancer Research (1916–1930) | The American Journal of Cancer (1931–1940)

Acquired *TNFRSF14* Mutations in Follicular Lymphoma Are Associated with Worse Prognosis

K-John J. Cheung, Nathalie A. Johnson, Joslynn G. Affleck, et al.

Cancer Res 2010;70:9166-9174. Published OnlineFirst September 30, 2010.